Development 138, 3273-3286 (2011) doi:10.1242/dev.066142

Crimpy inhibits the BMP homolog Gbb in motoneurons to enable proper growth control at the *Drosophila* neuromuscular junction

Rebecca E. James and Heather T. Broihier*

SUMMARY

The BMP pathway is essential for scaling of the presynaptic motoneuron arbor to the postsynaptic muscle cell at the *Drosophila* neuromuscular junction (NMJ). Genetic analyses indicate that the muscle is the BMP-sending cell and the motoneuron is the BMP-receiving cell. Nevertheless, it is unclear how this directionality is established as Glass bottom boat (Gbb), the known BMP ligand, is active in motoneurons. We demonstrate that *crimpy* (*cmpy*) limits neuronal Gbb activity to permit appropriate regulation of NMJ growth. *cmpy* was identified in a screen for motoneuron-expressed genes and encodes a single-pass transmembrane protein with sequence homology to vertebrate Cysteine-rich transmembrane BMP regulator 1 (Crim1). We generated a targeted deletion of the *cmpy* locus and find that loss-of-function mutants exhibit excessive NMJ growth. In accordance with its expression profile, tissue-specific rescue experiments indicate that *cmpy* functions neuronally. The overgrowth in *cmpy* mutants depends on the activity of the BMP type II receptor Wishful thinking, arguing that Cmpy acts in the BMP pathway upstream of receptor activation and raising the possibility that it inhibits Gbb activity in motoneurons. Indeed, the *cmpy* mutant phenotype is strongly suppressed by RNAi-mediated knockdown of Gbb in motoneurons. Furthermore, Cmpy physically interacts with the Gbb precursor protein, arguing that Cmpy binds Gbb prior to the secretion of mature ligand. These studies demonstrate that Cmpy restrains Gbb activity in motoneurons. We present a model whereby this inhibition permits the muscle-derived Gbb pool to predominate at the NMJ, thus establishing the retrograde directionality of the pro-growth BMP pathway.

KEY WORDS: *Drosophila melanogaster*, Motoneuron, Neuromuscular junction, Glass bottom boat, Crim1, BMP antagonist

INTRODUCTION

Motoneurons constitute a fundamental line of communication between the CNS and the periphery. In an anterograde direction, they integrate central interneuron inputs to appropriately depolarize postsynaptic muscle to trigger contractions and stimulate movement. In the retrograde direction, they translate information about muscle activity to modulate synaptic size and strength at the neuromuscular junction (NMJ). Thus, the NMJ is not only a location of neurotransmitter release, but also a primary site of action for pathways that foster communication between synaptic partners. Whereas the directionality of neurotransmission is defined by the inherent cellular asymmetry of pre- and postsynaptic compartments, the directionality of signaling pathway action at the synapse cannot be established in the absence of functional analyses of individual pathway components.

The Wingless/Wnt and bone morphogenetic protein (BMP) morphogens mediate coordinated differentiation of the motoneuron and the muscle cell at the *Drosophila* NMJ (McCabe et al., 2003; Packard et al., 2002). Forward and reverse genetic approaches have defined pathways that regulate the developmental expansion of the NMJ during larval development. Wingless is released from motoneuron terminals and binds to Frizzled 2 receptors on both the pre- and postsynaptic sides to stimulate NMJ growth and differentiation (Ataman et al., 2008; Miech et al., 2008; Packard et al., 2002). The BMP homolog Glass bottom boat (Gbb) has been proposed to act in a retrograde manner to regulate synaptic growth and function (McCabe et al., 2003). Gbb is postulated to be secreted from the muscle and to bind the type II BMP serine/threonine kinase receptor Wishful thinking (Wit) on presynaptic motoneuron terminals. The Gbb-Wit interaction drives recruitment and activation of a type I receptor – Saxophone (Sax) and/or Thickveins (Tkv) (Aberle et al., 2002; Allan et al., 2003; Marques et al., 2002; McCabe et al., 2004; McCabe et al., 2003; Rawson et al., 2003). Signal transduction within the motoneuron acts via phosphorylation of the R-Smad Mothers against decapentaplegic (Mad), the association of phospho-Mad with the co-Smad Medea (Med), and the translocation of this complex to the nucleus to elicit changes in gene transcription (Keshishian and Kim, 2004; Raftery and Sutherland, 1999).

Loss-of-function (LOF) mutants in BMP pathway components result in NMJ undergrowth and impaired basal synaptic transmission at the NMJ (Aberle et al., 2002; Marques et al., 2002; McCabe et al., 2004; McCabe et al., 2003; Rawson et al., 2003). Conversely, elevated BMP signaling, as found in LOF mutants for the inhibitory Smad Daughters against decapentaplegic (Dad) or in larvae expressing the constitutively active type I receptor Tkv, results in substantial expansion of the NMJ (O'Connor-Giles et al., 2008; Sweeney and Davis, 2002). Furthermore, identification of factors that modulate BMP signaling activity on the presynaptic side demonstrates that growth of the motoneuron arbor is exquisitely sensitive to neuronal levels of BMP signal transduction (Kim et al., 2010; O'Connor-Giles et al., 2008; Sweeney and Davis, 2002; Wang et al., 2007). Additionally, the BMP pathway might serve an anterograde or autocrine function in muscle, as Tkv and phospho-Mad are present in the postsynaptic compartment (Dudu et al., 2006).

Department of Neurosciences, Case Western Reserve University School of Medicine, Cleveland, OH 44106, USA.

*Author for correspondence (heather.broihier@case.edu)

Accepted 25 May 2011

However, a function has not been assigned to this pathway, as presynaptic, but not postsynaptic, expression of Mad, Med, Tkv, Sax and Wit rescues the anatomical NMJ defects in the corresponding LOF mutants (Aberle et al., 2002; McCabe et al., 2004). Hence, components of the BMP signal transduction cascade are required in motoneurons for developmental NMJ expansion.

Although a number of lines of evidence indicate that motoneurons receive a BMP signal, the source of the signal is less well established. The BMP homolog Gbb is postulated to act retrogradely on the basis of tissue-specific rescue experiments demonstrating that muscle-specific, but not neuron-specific, expression of Gbb in a hypomorphic *gbb* background rescues NMJ size and bouton number (McCabe et al., 2003). However, neurotransmitter release at the NMJ is not rescued strongly in these animals (Goold and Davis, 2007; McCabe et al., 2003). By contrast, basal neurotransmission is fully recovered when Gbb is expressed pan-neuronally in a *gbb*-deficient background (Goold and Davis, 2007; McCabe et al., 2003), suggesting the possibility of a presynaptic function for Gbb at the NMJ. Consistent with this model, Gbb is expressed ubiquitously in late embryos (McCabe et al., 2003). Moreover, a motoneuronal function for Gbb in larvae is strongly implied by functional studies demonstrating that Gbb acts retrogradely in motoneurons to strengthen synaptic transmission with their presynaptic partners. This elegant work established that motoneuronal Gbb is necessary and sufficient to facilitate synaptic excitation between larval motoneurons and presynaptic cholinergic interneurons (Baines, 2004).

We identified CG13253, which we named *crimpy* (*cmpy*), in a screen for embryonic motoneuron-expressed transcripts. *cmpy* is predicted to encode a cysteine-rich repeat (CRR)-containing single-pass transmembrane protein, with sequence homology to vertebrate Cysteine-rich transmembrane BMP regulator 1 (Crim1) (Kolle et al., 2000; Kolle et al., 2003; Wilkinson et al., 2003). CRRs are present in a large number of BMP-interacting proteins in vertebrates and invertebrates (Umulis et al., 2009; Walsh et al., 2010). This structurally related family includes extracellular antagonists, such as *Drosophila* Short gastrulation (Sog) and vertebrate Chordin (Chrd), which are believed to interfere with receptor-ligand interactions (Bachiller et al., 2000; Francois et al., 1994). It also includes proteins such as gremlin and sclerostin that can interact with BMPs intracellularly and are thought to interfere with BMP activity, at least in part, by altering ligand activation or secretion (Krause et al., 2010; Sun et al., 2006). Here, we present evidence that Cmpy is a novel antagonist of BMP signaling at the NMJ. We propose that Cmpy antagonizes motoneuronal Gbb activity to establish the retrograde directionality of the pro-growth Gbb signal, hence maintaining synchronization of presynaptic axon elaboration and postsynaptic muscle growth.

MATERIALS AND METHODS

Fly stocks

Stocks used include: *UAS-CG13253^{RNAi}*-KK library (transformant ID 101249; Vienna Drosophila RNAi Center); *elavGal4*, *D42Gal4* and *OK6Gal4* (A. DiAntonio, Washington University, St Louis, MO, USA); *Mad^{1}* and *A9Gal4* (K. O'Connor-Giles, University of Wisconsin, Madison, WI, USA); *gbb^{1}* and *UAS-gbb(9.9)* (B. McCabe, Columbia University, New York, NY, USA); and *UAS-gbb^{RNAi}* (K. Wharton, Brown University, Providence, RI, USA). *UAS-cmpy* transgenic flies were generated by BestGene. All other stocks were obtained from Bloomington Stock Center.

Identification of CG13253 and allele generation

To identify uncharacterized genes with neuronal expression, an in silico screen of the FlyExpress expression pattern database was performed. We were interested in transcripts with embryonic nerve cord expression patterns that were not pan-neuronal, with the goal of identifying genes that act in functionally related neuronal populations. We obtained ESTs from the Drosophila Genomics Resource Center for genes with apparent expression in specific neuronal subtypes and analyzed their RNA expression patterns.

To generate a null allele of CG13253, targeted recombination between FRT site-containing *piggyBac* (*PBac*) elements was utilized (Parks et al., 2004; Thibault et al., 2004). In the presence of FLP recombinase, recombination between the FRT sites of heterozygous *PBac* elements in trans in germline stem cells can lead to the recovery of progeny carrying deletions for the genomic region flanked by the two *PBac* elements. The resulting progeny will contain a hybrid *PBac* element containing portions of each parental P-element. In this manner, a ~8 kb region was deleted between *PBac{WH}f02482* and *PBac{WH}f01736* at 77E3 on chromosome 3L (CG13253Δ8; Fig. 1F). Four approaches were utilized to verify the CG13253Δ8 deletion: (1) PCR to amplify from each side of the resulting hybrid *PBac* into genomic DNA verified the presence of portions of both elements within the same genetic background, indicating a recombination event (data not shown); (2) genomic primers targeting the putatively deleted region were used to PCR amplify a ~3 kb band from Oregon R (OR) DNA that was absent from CG13253Δ8 homozygous DNA (data not shown); (3) PCR with genomic primers flanking the resultant hybrid *PBac* verified the deletion by demonstrating the size difference in the intervening DNA between OR and CG13253Δ8 homozygous DNA (Fig. 1G); and (4) in situ hybridization analysis of CG13253 homozygous mutant embryos revealed an absence of CG13253 mRNA (Fig. 1H).

A second gene, CG34260, is annotated within the CG13253 locus on FlyBase and is present within the 8 kb region. CG34260 is located on the opposite DNA strand to CG13253 and is predicted to encode a 219 amino acid protein. No CG34260 ESTs have been identified. We generated an antisense RNA probe to CG34260 and did not detect embryonic expression (data not shown). Since CG13253 RNAi phenocopies the NMJ phenotype displayed by CG13253Δ8 homozygotes, and a CG13253 transgene rescues the NMJ phenotype in deletion animals, we conclude that the NMJ phenotypes present in deletion animals result from loss of CG13253 function.

Immunohistochemistry

Embryo fixation, in situ hybridization and immunohistochemistry were carried out as previously described (Miller et al., 2008). For all larval experiments, ten virgin females were crossed to five males, and bottles were maintained at 25°C for 4 days before removing adults. Dissection of wandering third instar larvae was carried out in ice-cold PBS, and body walls were fixed in Bouin's Fixative (Polysciences). The following primary antibodies were used: rabbit anti-Hb9 (Exex – FlyBase) at 1:1000 (Broihier and Skeath, 2002), rabbit anti-Eve at 1:1000 (M. Frasch, Mt Sinai Medical Center, New York, NY, USA), mAb 1D4 at 1:10 [anti-Fasciclin II; Developmental Studies Hybridoma Bank (DSHB)], rabbit anti-HRP at 1:300 (Jackson Laboratories), mouse anti-Dlg at 1:1000 (DSHB), mouse anti-NC82 (Bruchpilot) at 1:100 (DSHB), rabbit anti-Nwk at 1:1000 (K. O'Connor-Giles), and rabbit anti-GluRIII (GluRIIC – FlyBase) at 1:5000 (A. DiAntonio).

Imaging and data analysis

Embryos and larvae were analyzed on a Zeiss Axioplan 2 microscope using 40×, 63× and 100× oil-immersion objectives. Fluorescence images of larval body walls were obtained with a Zeiss Axio Imager.Z1 confocal microscope at 40×. Brightness and contrast were adjusted in Adobe Photoshop CS5. Quantification of type I glutamatergic boutons was carried out at NMJ 6/7 and NMJ 4. The muscle area of all genotypes analyzed was similar. For NMJ 6/7, boutons were quantified at both segment A2 and segment A3. Although consistent results were obtained for all experiments at A3, only data for NMJ 6/7 in A2 are presented because of segment-specific differences. The data presented for NMJ 4 are pooled from both A2 and A3. Groups of means were compared by one-way ANOVA, and the unpaired Student's *t*-test was used for comparisons between pairs of means.

Plasmids

EST clones for *cmpy* (RE53920) and *gbb* (GH12092) and pAWF C-terminal 3× Flag and pAWH C-terminal 3× HA tag Gateway System (Invitrogen) compatible vectors were obtained from the Drosophila

Genomics Resource Center. Vectors pDEST-GBKT7 and pDEST-GADT7 (Rossignol et al., 2007) for yeast two-hybrid analysis were obtained from the Arabidopsis Biological Resource Center. For immunoprecipitations, full-length *cmpy* and *gbb* coding sequences in the pCR8/GW/TOPO vector (Invitrogen) were cloned into pAWF or pAWH destination vectors with Gateway Long-Range Clonase II Enzyme Mix according to the manufacturer's protocols (Invitrogen). For yeast two-hybrid experiments, domains were subcloned into pDEST-GADT7 (*cmpy* constructs, prey) or pDEST-GBKT7 (*gbb* constructs, bait). Immunoprecipitation and yeast two-hybrid experiments were carried out as previously described (Weng et al., 2011).

RESULTS

CG13253 encodes a predicted single-pass transmembrane protein expressed in the CNS

CG13253 was identified in a screen for embryonic motoneuron-expressed transcripts in the ventral nerve cord (VNC) (see Materials and methods). CG13253 RNA expression initiated at stage 13 in clusters of medial and lateral postmitotic neurons in the VNC. At embryonic stage 14, it was expressed in a segmentally repeated V-shaped pattern (Fig. 1A) that is reminiscent of the expression profile of Hb9, a marker for ventrally and laterally projecting motoneurons (Fig. 1B) (Broihier and Skeath, 2002; Odden et al., 2002). Indeed, CG13253 was expressed in a subset of Hb9-positive neurons, including the ventrally projecting RP motoneurons (Fig. 1C), as well as in dorsally projecting Even skipped (Eve)-positive motoneurons (data not shown) (Landgraf et al., 1999). The CG13253 expression domain expanded at stage 15, and by the end of embryogenesis it was widely expressed in the VNC (Fig. 1D). In the embryo, appreciable CG13253 expression was not detected outside of the VNC (data not shown). Hence, CG13253 is expressed in dorsally and ventrally projecting motoneuron populations, although the large number of CG13253-positive cells in the VNC indicates that its expression is not motoneuron specific.

CG13253 is predicted to encode a single-pass 273 amino acid type II transmembrane protein with an insulin-like growth factor binding protein (IGFBP)-like domain and a single low-threshold CRR (Fig. 1E). There is also an arginine/lysine-rich domain at the C-terminus. CG13253 shares homology with vertebrate Crim1 (Kolle et al., 2000; Kolle et al., 2003), which encodes a single-pass transmembrane protein with an N-terminal IGFBP-like domain, a short C-terminal cytoplasmic tail, and six CRRs interspersed between the IGFBP motif and the putative transmembrane domain (Kolle et al., 2000). Crim1 is expressed in early populations of motoneurons and interneurons in the developing mouse, although its neuronal function remains obscure (Wilkinson et al., 2003).

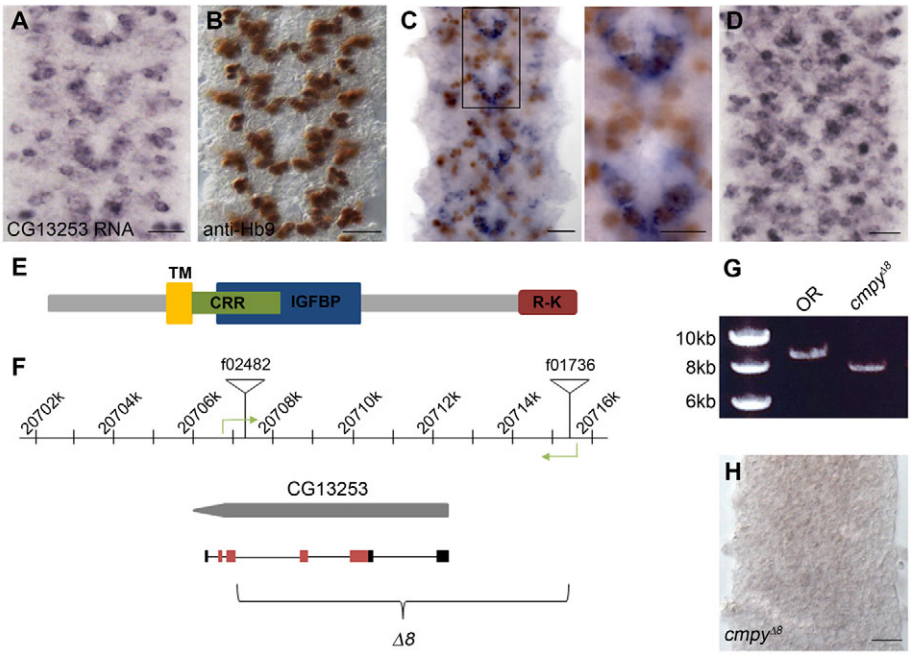

Fig. 1. *Drosophila* CG13253 expression analysis and allele generation. (**A-D**) Wild-type (Oregon R) embryonic ventral nerve cord (VNC) labeled with the indicated markers. CG13253 mRNA is expressed in a segmentally repeating V-shaped pattern at stage 14 (A), similar to the expression profile of Hb9 (B). (C) CG13253 mRNA (purple) is co-expressed with a subset of $Hb9^{+}$ cells (brown). The boxed region is shown at a higher magnification to the right. The double-labeled cells correspond to the cluster of RP motoneurons. (D) At stage 16, CG13253 mRNA is widely expressed in the VNC. (**E**) Predicted domain structure of the CG13253 protein product. TM, transmembrane domain; CRR, cysteine-rich repeat; IGFBP, insulin-like growth factor binding protein-like domain; R-K, arginine/lysine-rich domain. The predicted CRR and IGFBP domains overlap. (**F**) Genomic organization of the CG13253 locus. The CG13253 coding sequence is indicated in gray and the mRNA is shown beneath; black and red boxes are untranslated and coding regions, respectively, and introns are depicted as thin black lines. Inverted triangles indicate the *piggyBac* (*PBac*) elements utilized to generate the deletion allele $cmpy^{\Delta 8}$. Green arrows show the location of genomic primers used to verify the deletion. (**G**) PCR using the primers shown in F verifies deletion of most of the coding region of CG13253. Amplification in a wild-type, non-*PBac*-containing background yields an 8.89 kb product (lane OR), whereas amplification across the hybrid *PBac* that remains following recombination yields a 7.86 kb product (lane $cmpy^{\Delta 8}$). (**H**) CG13253 mRNA is not expressed in the VNC of $cmpy^{\Delta 8}$ homozygous mutant embryos. Scale bars: 20 μm, except 10 μm in right-hand panel of C.

CG13253 (*crimpy*) functions in motoneurons to restrict NMJ growth

To investigate CG13253 function in neuronal development, a LOF allele was generated by targeted recombination between *piggyBac* (*PBac*) elements in trans (Parks et al., 2004). In this manner, we generated an 8 kb deletion (CG13253Δ8) that includes ~3 kb of upstream sequence, the translation initiation site and the majority of the coding sequence (Fig. 1F). Deletion was verified by multiple strategies (see Materials and methods), including amplification across the deletion with genomic primers to either side of the resulting hybrid *PBac* element. Amplification in a wild-type, non-*PBac*-containing background yielded an 8.89 kb product, whereas amplification across the hybrid *PBac* that remained following recombination yielded a 7.86 kb product comprising 7.23 kb of hybrid *PBac* and 630 bases of genomic DNA (Fig. 1G). Consistent with the presence of the deletion, CG13253 RNA was not expressed in homozygous deletion embryos (Fig. 1H), indicating that this deletion represents a null allele. CG13253Δ8 mutants were viable, although the homozygous females were sterile. In accordance with characteristics of the mutant phenotype described below and the sequence similarity of CG13253 to vertebrate *Crim1*, we named this gene *crimpy* (*cmpy*), and refer to the LOF allele as $cmpy^{\Delta 8}$.

Since *cmpy* is expressed in motoneurons when cell fate and motor axon guidance decisions occur, we tested whether *cmpy* regulates these processes. We did not observe defects in neuronal cell fate acquisition or axon guidance in *cmpy* homozygotes, as assessed by cell fate markers Eve and Hb9 and axonal marker mAb 1D4 (data not shown) (Broihier and Skeath, 2002; Landgraf et al., 1999; Van Vactor et al., 1993). These results suggest that *cmpy* does not contribute to motoneuron cell fate specification or axon guidance, motivating us to examine later stages of motoneuron differentiation.

The fly NMJ serves as an ideal model for the investigation of synaptic development and function (Collins and DiAntonio, 2007). Since *cmpy* is expressed in motoneurons, we asked whether *cmpy* mutants exhibit defects in NMJ development. We scored all type I glutamatergic boutons (Johansen et al., 1989) at two well-characterized, identifiable NMJs – the NMJ that innervates the cleft between muscles 6 and 7 (NMJ 6/7) and the NMJ on the face of muscle 4 (NMJ 4). $cmpy^{\Delta 8}$ homozygotes displayed a 52% increase in the number of boutons at NMJ 6/7 and a 57% increase in type I boutons at NMJ 4 (Fig. 2A-D,I,J; Table 1), indicating that *cmpy* restrains NMJ growth. We observed comparably increased bouton number in $cmpy^{\Delta 8}/Df(3L)452$ larvae (Fig. 2I,J; Table 1), supporting the conclusion that $cmpy^{\Delta 8}$ is a null allele. Type I boutons are

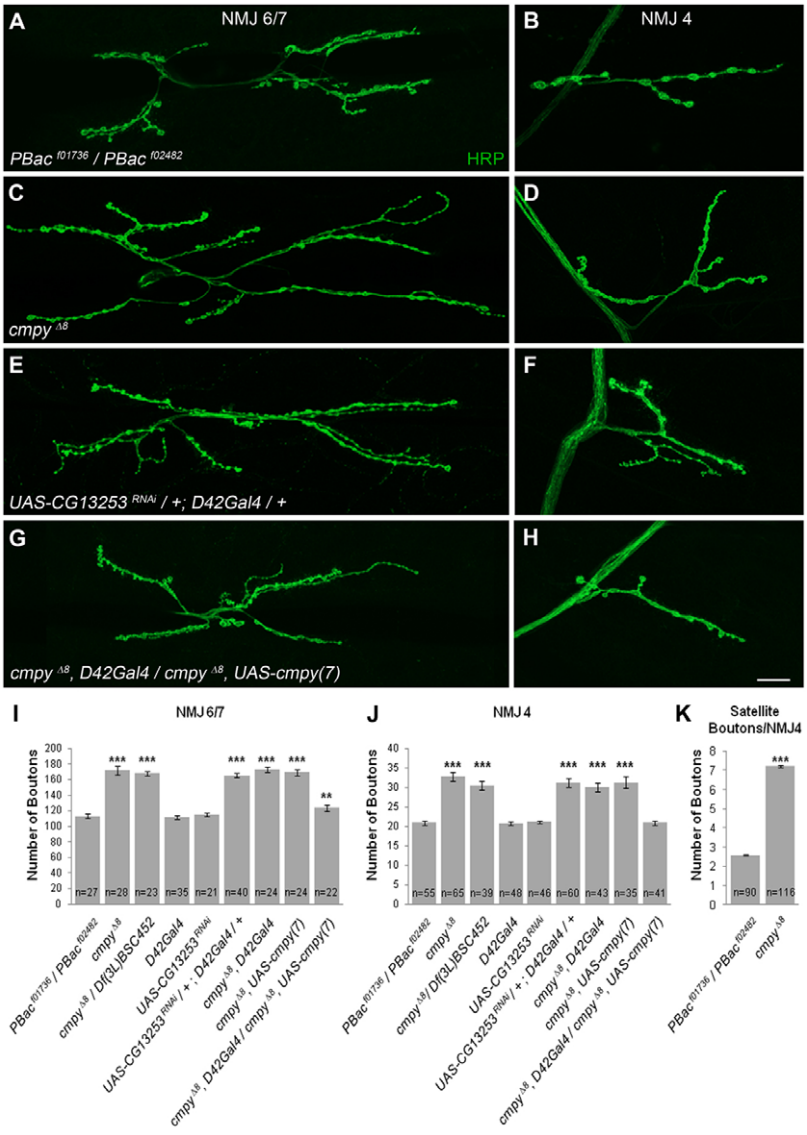

Fig. 2. *cmpy* functions in motoneurons to attenuate NMJ expansion. (**A-H**) Representative confocal images of *Drosophila* NMJ 6/7 (A,C,E,G) and NMJ 4 (B,D,F,H) of the indicated genotypes labeled with the neuronal membrane label anti-HRP. (A,B) Wild type corresponds to heterozygous parental *PBac* elements, $PBac^{f01736}/PBac^{f02482}$. (C,D) $cmpy^{\Delta 8}$ homozygous NMJs display an increase in the total number of type I synaptic boutons. (E,F) RNAi-mediated knockdown of *cmpy* mRNA in motoneurons gives statistically indistinguishable overgrowth as observed at $cmpy^{\Delta 8}$ NMJs. (G,H) Motoneuronal overexpression of *cmpy* in the $cmpy^{\Delta 8}$ background restores proper growth regulation. The rescue is complete at NMJ 4 and partial at NMJ 6/7. (**I**,**J**) Quantification of the mean number of type I boutons per indicated genotype at NMJ 6/7 and NMJ 4. The number of NMJs scored per genotype (*n*) is indicated within the bars. (**K**) Mean number of satellite boutons at NMJ 4. Statistical comparisons are to wild type unless otherwise indicated. Error bars indicate s.e.m. **, $P<0.01$; ***, $P<0.001$. Raw data are found in Table 1. Scale bar: 20 μm.

Table 1. *cmpy* loss-of-function and BMP genetic interaction phenotypes at the NMJ

	NMJ 6/7 (A2)		NMJ 4 (A2 + A3)	
Genotype	*n*	Total boutons	*n*	Total boutons
PBac^{f01736}/PBac^{f02482}	27	113.3±2.4	55	20.9±0.5
cmpy$^{\Delta 8}$	28	171.9±5.9	39	32.8±1.1
cmpy$^{\Delta 8}$/Df(3L)BSC452	23	168.1±3.0	39	30.5±1.2
D42Gal4	36	111.3±2.0	48	20.9±0.4
UAS-CG13253^{RNAi}	21	115.3±2.4	46	21.2±0.4
UAS-CG13253^{RNAi}/+, D42Gal4/+	40	161.4±2.8	60	31.3±1.5
cmpy$^{\Delta 8}$, D42Gal4	24	172.9±3.1	43	30.1±1.1
cmpy$^{\Delta 8}$, elavGal4	22	172.1±3.5	39	35.0±1.9
cmpy$^{\Delta 8}$, UAS-cmpy(4)	11	159.2±7.1	17	31.6±2.2
cmpy$^{\Delta 8}$, UAS-cmpy(7)	24	169.4±4.0	35	31.3±1.4
cmpy$^{\Delta 8}$, D42Gal4/cmpy$^{\Delta 8}$, UAS-cmpy(7)	22	123.9±3.8	41	21.0±0.6
cmpy$^{\Delta 8}$, elavGal4/cmpy$^{\Delta 8}$, UAS-cmpy(4)	12	131.8±6.7	17	22.3±1.1
cmpy$^{\Delta 8}$, elavGal4/cmpy$^{\Delta 8}$, UAS-cmpy(7)	45	128.0±3.0	35	20.6±0.9
gbb^{1}/+	24	121.0±2.5	39	20.9±0.7
Mad^{1}/+	24	117.7±2.8	38	20.2±0.5
wit^{A12}/+	19	120.5±3.8	35	21.1±0.6
gbb^{1}/+; cmpy$^{\Delta 8}$	23	143.8±3.3	37	24.7±0.8
Mad^{1}/+; cmpy$^{\Delta 8}$	28	147.1±3.4	40	26.2±1.1
wit^{A12}, cmpy$^{\Delta 8}$/+, cmpy$^{\Delta 8}$	29	148.0±2.7	46	25.2±0.9
wit^{A12}/wit^{B11}	19	69.7±5.0	29	11.2±1.6
wit^{A12}; cmpy$^{\Delta 8}$	31	76.0±2.7	43	11.8±0.8

n, the number of NMJs scored per genotype; data represent two or more experiments pooled.

further classified into two types based on their size and the extent of the Discs large (Dlg)-positive postsynaptic subsynaptic reticulum (SSR) (Atwood et al., 1993; Lahey et al., 1994). Type Ib (big) boutons are surrounded by a prominent Dlg-positive SSR, whereas the Dlg-positive SSR enveloping type Is (small) boutons is less extensive. Although *cmpy* mutant boutons tended to be smaller than those of the wild type, the overall proportion with strong Dlg immunofluorescence appeared unchanged (data not shown), arguing that *cmpy* does not selectively regulate the development of type Ib or type Is boutons. We further quantified the number of satellite boutons at NMJ 4 in *cmpy* homozygotes (Dickman et al., 2006; O'Connor-Giles et al., 2008). We define satellite boutons as small boutons present on short branches (three or fewer boutons) distinct from primary arbors, or as single boutons that bud off of primary boutons without an intervening axon segment. *cmpy* mutants displayed a 2.9-fold increase in the number of satellite boutons at NMJ 4 (Fig. 2K). A comparable increase in satellite bouton formation is observed in mutants with elevated levels of BMP signaling (O'Connor-Giles et al., 2008). The presence of numerous small boutons in *cmpy* mutants is reminiscent of a type of rock climbing route featuring small holds, or crimps, which can be described as a 'crimpy' route.

Since *cmpy* encodes a neuronal transcript, a straightforward hypothesis is that *cmpy* acts in motoneurons to inhibit NMJ growth. We utilized the GAL4/UAS transactivation system (Brand and Perrimon, 1993) to evaluate the ability of RNAi-mediated knockdown of *cmpy* to recapitulate the *cmpy$^{\Delta 8}$* overgrowth phenotype. Using the larval motoneuron driver *D42Gal4* (Sanyal, 2009), we found 47% and 49% increases in bouton number at NMJ 6/7 and NMJ 4, respectively, in *D42>cmpy^{RNAi}* larvae as compared with controls (Fig. 2A,B,E,F,I,J; Table 1). We observed comparable increases in bouton number using the pan-neuronal driver *elavGal4* to drive *cmpy* RNA knockdown (data not shown).

The NMJ overgrowth displayed by animals with neuron-specific *cmpy* knockdown argues that *cmpy* acts presynaptically. As a key test of this hypothesis, we performed tissue-specific rescue experiments. Since neuronal *cmpy* overexpression in an otherwise wild-type background does not alter NMJ growth (Table 2), we

Table 2. Gbb and Cmpy gain-of-function phenotypes at the NMJ

	NMJ 6/7 (A2)		NMJ 4 (A2 + A3)	
Genotype	*n*	Total boutons	*n*	Total boutons
D42Gal4	36	111.3±2.0	48	20.9±0.4
UAS-gbb(9.9)	21	115.2±2.8	34	20.9±0.5
UAS-cmpy(3), UAS-gbb(9.9)	25	112.2±3.2	39	20.9±0.6
UAS-gbb(9.9), UAS-lacZ	21	116.2±2.2	38	21.3±0.7
UAS-gbb(9.9)/+; D42Gal4/+	24	157.4±3.9	41	33.9±1.9
UAS-cmpy(3), UAS-gbb(9.9)/+; D42Gal4/+	24	115.0±2.5	37	21.2±1.1
UAS-gbb(9.9), UAS-lacZ/+; D42Gal4/+	23	149.7±3.6	24	50.8±2.7
elavGal4	23	119.8±1.8	34	20.3±0.7
24BGal4	20	123.1±1.9	24	21.0±0.4
UAS-cmpy(3)	29	127.1±2.3	43	20.7±0.4
UAS-cmpy(3)/+; elavGal4/+	34	125.2±2.0	44	19.9±0.4
UAS-cmpy(3)/+; 24BGal4/+	21	100.5±2.5	32	16.3±0.7

n, the number of NMJs scored per genotype; data represent two or more experiments pooled.

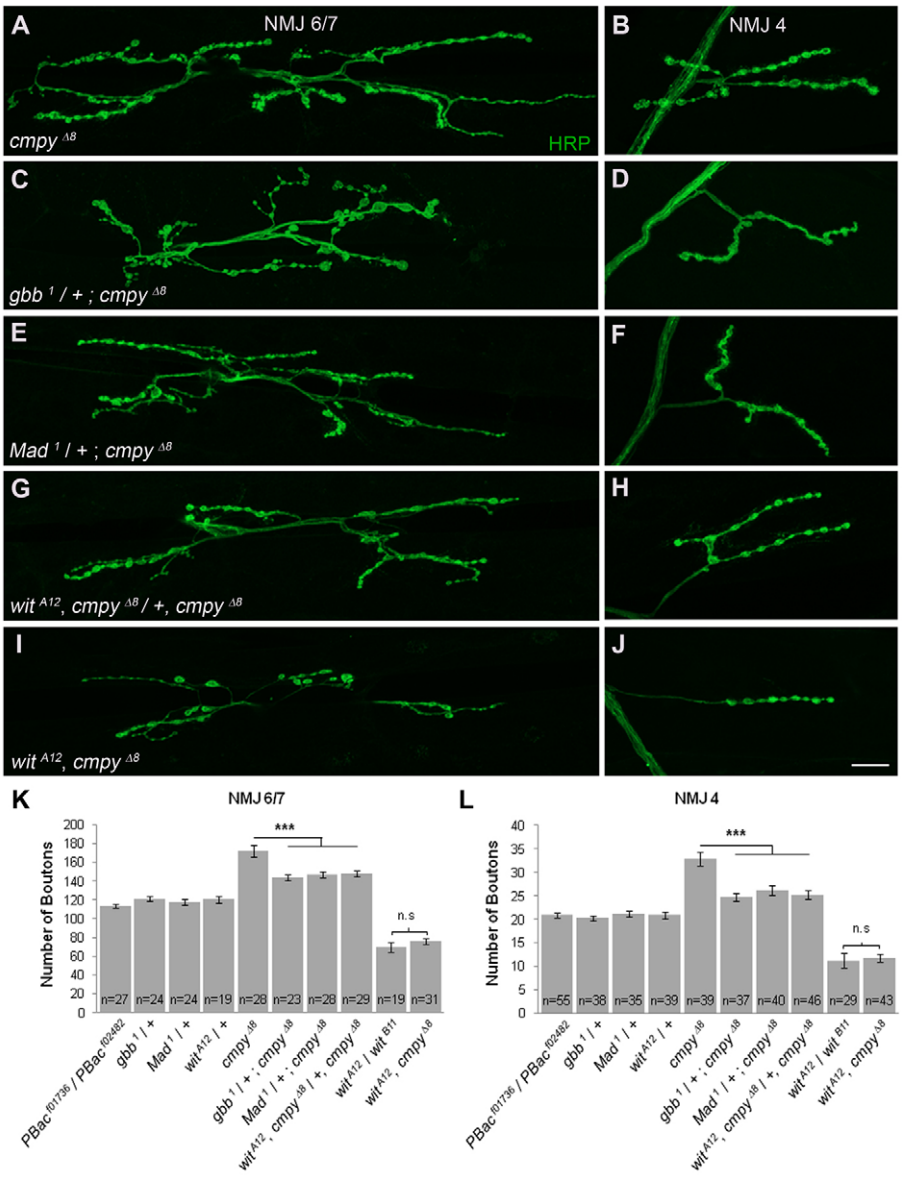

Fig. 3. *cmpy* acts in the BMP signaling pathway upstream of the BMP type II receptor *wit*. (**A-J**) Representative confocal images of *Drosophila* NMJ 6/7 (A,C,E,G,I) and NMJ 4 (B,D,F,H,J) labeled with anti-HRP. (A,B) $cmpy^{\Delta 8}$ NMJs display an increase in type I boutons. Loss of one copy of *gbb* (C,D), *Mad* (E,F) or *wit* (G,H) results in partial suppression of the increase in bouton number in $cmpy^{\Delta 8}$ mutants. The reduction in type I bouton number at *wit* mutant NMJs (G,H) matches the reduction observed at *wit cmpy* double-mutant NMJs (I,J). (**K**,**L**) Quantification of the mean number of type I boutons per genotype at NMJ 6/7 and NMJ 4. Statistical comparisons are to wild type unless otherwise indicated. Error bars represent s.e.m. ***, $P<0.001$; n.s., not significant. Raw data are found in Table 1. Scale bar: 20 μm.

examined whether *D42Gal4*-mediated overexpression of *cmpy* in a *cmpy* homozygous background rescues proper regulation of NMJ growth. At NMJ 4, proper bouton number was fully rescued, whereas at NMJ 6/7 overgrowth was reduced from 52% in *cmpy* homozygotes to 9% in *cmpy* homozygotes with motoneuronal *cmpy* expression (Fig. 2G-J; Table 1). Comparable rescue was observed using *elavGal4* to drive *cmpy* in all neurons (Table 1). Thus, *cmpy* acts in motoneurons to limit NMJ arbor expansion during development.

In addition to characterizing NMJ growth, we analyzed synaptic structure in $cmpy^{\Delta 8}$ larvae. To evaluate active zone formation, we used an antibody against Bruchpilot (Wagh et al., 2006) to label active zones. Indeed, *cmpy* mutant NMJs contained more active zones. However, the percentage increase was comparable to that in bouton number, so that the active zone density remains constant (data not shown). Furthermore, the assembly of periactive zones, as evidenced by localization of the endocytic adaptor Nervous wreck (Nwk), appeared normal in *cmpy* mutants (data not shown). On the postsynaptic side, an antibody to the glutamate receptor subunit GluRIII (Marrus et al., 2004) was utilized to mark glutamate receptor clusters. We did not detect a change in glutamate receptor distribution in *cmpy* mutants (data not shown). Hence, *cmpy* does not appear to function selectively in synapse assembly or maturation, but rather appears necessary for the regulation of a general NMJ growth-promoting program.

cmpy is genetically upstream of the BMP type II receptor *wit*

The BMP pathway has emerged as a crucial positive regulator of NMJ growth. LOF mutants in multiple pathway components, including *gbb*, *wit*, *tkv*, *sax*, *Mad* and *Med*, all exhibit small NMJs with reduced numbers of boutons (Aberle et al., 2002; Marques et al., 2002; McCabe et al., 2003; McCabe et al., 2004; Rawson et al., 2003). Conversely, those with elevated BMP activity, such as mutants for the inhibitory Smad *Dad*, display NMJ overgrowth, arguing that levels of BMP activity instruct arbor expansion (O'Connor-Giles et al., 2008; Sweeney and Davis, 2002).

To evaluate whether the increased number of boutons present in *cmpy* mutants reflects BMP pathway dysregulation, we tested if the *cmpy* LOF mutant phenotype is dominantly suppressed by

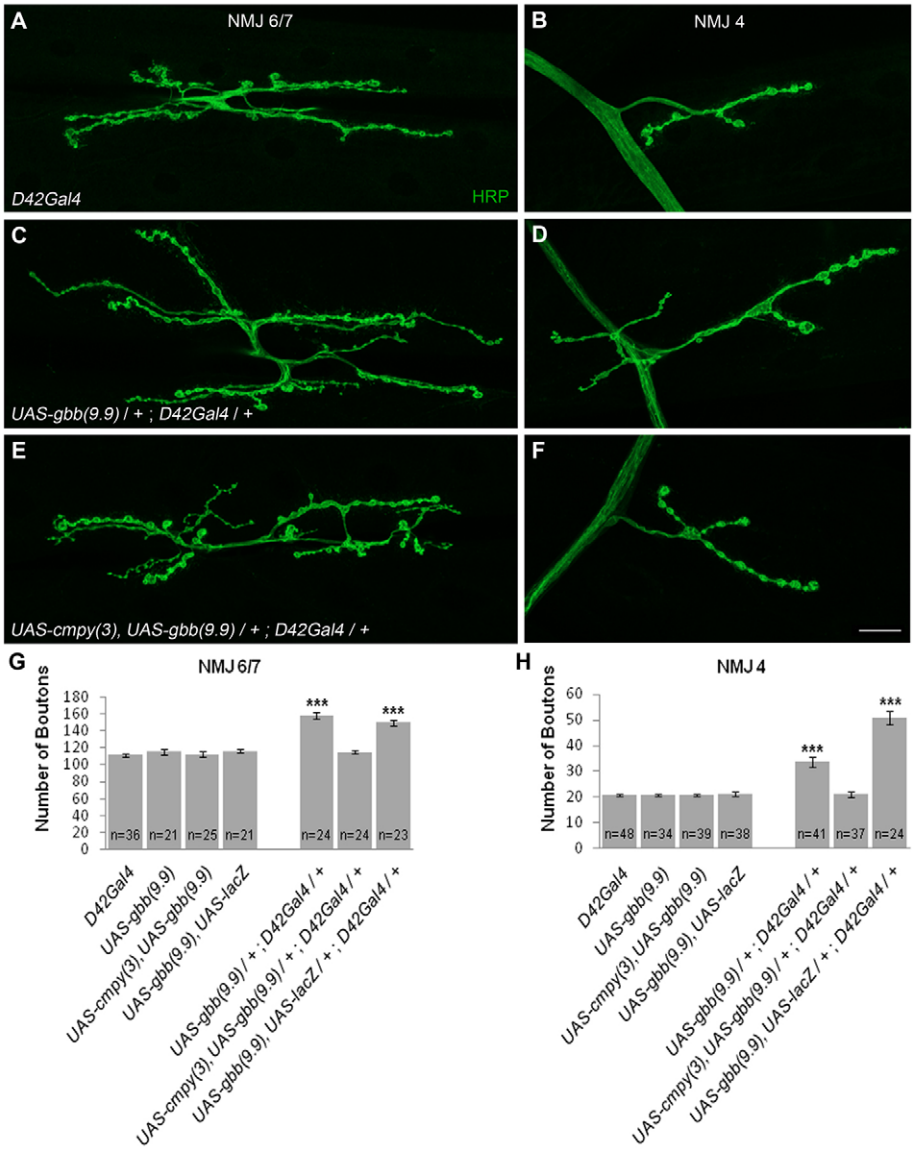

Fig. 4. Overexpression of *cmpy* suppresses NMJ expansion in larvae overexpressing neuronal *gbb*. (**A-F**) Representative confocal images of *Drosophila* NMJ 6/7 (A,C,E) and NMJ 4 (B,D,F) labeled with anti-HRP. (A,B) Wild type corresponds to *D42Gal4*. (C,D) Motoneuronal *gbb* overexpression promotes an increase in bouton number at NMJ 6/7 and NMJ 4. (E,F) *cmpy* overexpression completely suppresses overgrowth in motoneurons overexpressing Gbb at NMJ 6/7 and NMJ 4. (**G**,**H**) Quantification of the mean number of type I boutons per genotype at NMJ 6/7 and NMJ 4. The Gbb-induced overgrowth phenotype is not suppressed by co-overexpression of Gbb and *lacZ*. Statistical comparisons are to wild type unless otherwise indicated. Error bars represent s.e.m. ***, $P<0.001$. Raw data are found in Table 2. Scale bar: 20 μm.

LOF mutations in genes with pro-BMP activity. The BMP ligand *gbb*, the type II receptor *wit* and the transcription factor *Mad* are essential for BMP signaling at the NMJ, and NMJs in corresponding LOF homozygotes are undergrown (Aberle et al., 2002; Marques et al., 2002; McCabe et al., 2003; Rawson et al., 2003). We did not observe defects in NMJ expansion in *gbb*, *wit* or *Mad* heterozygotes, yet the overgrowth observed in *cmpy* mutants was suppressed by loss of one wild-type copy of *gbb*, *wit* or *Mad* (Fig. 3A-H,K,L; Table 1). For example, at NMJ 6/7, the percentage increase in bouton number fell from 52% in *cmpy* homozygotes to 24% in *cmpy* mutants lacking one copy of either *wit* or *Mad*, and to 20% with loss of one copy of *gbb*. These data argue that *cmpy* attenuates NMJ expansion by inhibiting BMP pathway activity.

Although these experiments place *cmpy* in the BMP pathway, they do not address the order of gene action. Thus, we conducted a classic genetic epistasis experiment to determine whether the increase in bouton number displayed by *cmpy* LOF mutants depends on activity of the BMP type II receptor *wit*. *wit cmpy* double mutants phenocopied the NMJ undergrowth displayed by *wit* single mutants (Fig. 3I-L; Table 1). For example, *wit* mutants exhibited a 46% reduction in bouton number at NMJ 4 compared with 44% in *wit cmpy* double mutants. Hence, *wit* mutants fully suppress the NMJ overgrowth observed in *cmpy* mutants, placing *cmpy* genetically upstream of *wit* in a common pathway. Since *cmpy* regulates NMJ growth upstream of BMP receptor activity, we probed the relationship between *cmpy* and the BMP ligand *gbb*.

cmpy overexpression blunts the phenotypic consequences of *gbb* overexpression

Muscle-specific expression of Gbb rescues the reduction in bouton number exhibited by *gbb* LOF mutants, demonstrating that the pathway can act in a retrograde direction (McCabe et al., 2003). However, Gbb expression is not muscle specific (McCabe et al., 2003). In particular, Gbb functions in the VNC (Baines, 2004). Motoneuronal Gbb poses a potential dilemma for models of retrograde BMP signaling at the NMJ. If Gbb constitutes the critical extracellular cue informing the presynaptic motoneuron about the size of its postsynaptic muscle partner, then it would appear crucial for the motoneuron to perceive primarily the muscle-derived Gbb pool to properly regulate growth. If Gbb were secreted from the motoneuron terminal, it would effectively dilute the

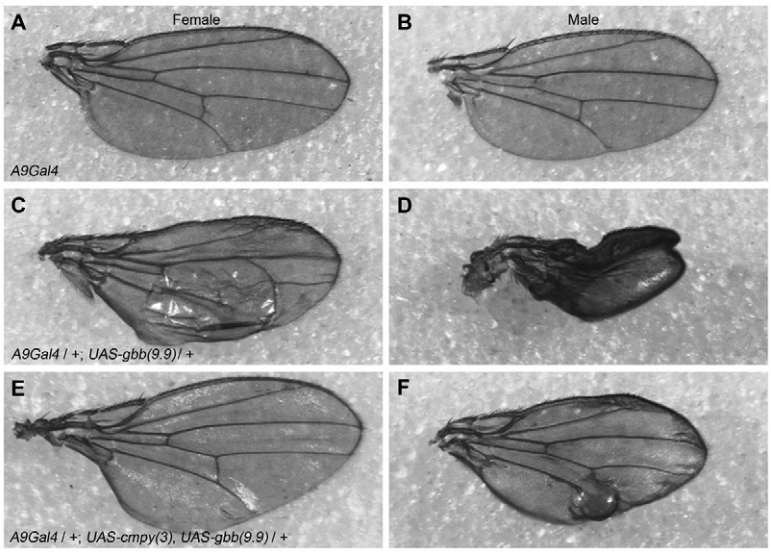

Fig. 5. Overexpression of *cmpy* suppresses *gbb* overexpression phenotypes in the wing disc. (**A-F**) Representative micrographs of wings from female (A,C,E) and male (B,D,F) flies; anterior is up and distal is to the right. (A,D) Wild type corresponds to *A9Gal4*. (B,E) Overexpression of Gbb using the wing imaginal disc driver *A9Gal4* results in a blistering phenotype in the posterior compartment of wings in females, and in males results in a more severe phenotype in which wings are blistered and remain unfurled. (C,F) Co-overexpression of Cmpy with Gbb suppresses the blistering phenotype in females and reduces the severity of the phenotype in males, such that wings are unfurled with mild blistering. Raw data are found in Table 3.

muscle-derived pool and potentially decouple pre- and postsynaptic growth. Hence, we reasoned that motoneurons might possess a cellular mechanism to modulate or inhibit Gbb at the NMJ.

As a test of this hypothesis, we overexpressed Gbb with the motoneuron driver *D42Gal4* and assessed NMJ morphology. *D42Gal4/UAS-gbb* larvae exhibited 40% and 62% increases in bouton number at NMJs 6/7 and 4, respectively (Fig. 4A-D,G,H; Table 2). Bouton numbers were comparably increased when Gbb was overexpressed via the *OK6Gal4* motoneuron driver (data not shown). This overgrowth argues that excess Gbb in motoneurons overwhelms growth regulatory mechanisms at the NMJ. Genetic epistasis experiments place *cmpy* in the BMP pathway upstream of the *wit* receptor, arguing that *cmpy* might inhibit *gbb*. Thus, we examined whether *cmpy* overexpression suppresses *gbb*-dependent NMJ overgrowth. Remarkably, co-overexpression of *cmpy* and *gbb* in motoneurons with either the *D42Gal4* or *OK6Gal4* driver resulted in NMJs with wild-type numbers of type I boutons at both NMJ 6/7 and NMJ 4 (Fig. 4E-H; Table 2; data not shown). The Gbb overexpression phenotype was not suppressed by co-overexpression of *lacZ*, indicating that suppression is mediated by Cmpy (Fig. 4G,H; Table 2). Importantly, neuronal *cmpy* overexpression did not inhibit NMJ growth in an otherwise wild-type background (Table 2), indicating that the suppression reflects an intimate relationship between Gbb and Cmpy and is not a secondary consequence of generic Cmpy-dependent growth inhibition. Neuronal Gbb overexpression is likely to drive excessive NMJ growth by an autocrine mechanism. Cmpy-dependent suppression of this phenotype argues that Cmpy inhibits the growth-promoting activity of Gbb in motoneurons.

To examine whether the Gbb-inhibiting activity of Cmpy is motoneuron specific, we investigated the ability of *cmpy* to antagonize *gbb* activity in an independent cellular context. Overexpression of Gbb in the developing wing disc results in a wing blistering phenotype (Khalsa et al., 1998). We found that Gbb overexpression in the wing disc with *A9Gal4* results in a blistering phenotype in 79% of females and in a more severe phenotype, including unfurling and blistering of the wing, in 93% of males (Fig. 5A-D; Table 3). Co-misexpression of *cmpy* and *gbb* strongly suppressed the blistering phenotype: only 11% of *A9Gal4/UAS-gbb, UAS-cmpy* females had blistered wings, and in males the severity of the unfurling/blistering phenotype was lessened, such that 89% of males exhibited wing blistering and only 11% exhibited unfurling of the wing and blistering (Fig. 5E,F; Table 3). The suppression is specific, as wing phenotypes were not suppressed by co-overexpression of *lacZ* (Table 3). Hence, *cmpy* overexpression suppresses *gbb*-dependent phenotypes in two cellular contexts: larval motoneurons and the wing imaginal disc.

Table 3. Gbb and Cmpy gain-of-function phenotypes in the wing

	Wing phenotype (%)*					
	Females			Males		
Genotype	WT	B	B/U	WT	B	B/U
A9Gal4	100 (156/156)	0	0	100 (155/155)	0	0
UAS-cmpy(3)	100 (81/81)	0	0	100 (85/85)	0	0
UAS-gbb(9.9)	100 (156/156)	0	0	100 (161/161)	0	0
UAS-cmpy(3), UAS-gbb(9.9)	100 (100/100)	0	0	100 (130/130)	0	0
UAS-gbb(9.9), UAS-lacZ/+	100 (100/100)	0	0	100 (100/100)	0	0
A9Gal4/+; UAS-cmpy(3)/+	100 (100/100)	0	0	100 (82/82)	0	0
A9Gal4/+; UAS-gbb(9.9)/+	21.4 (34/159)	78.6 (125/159)	0	0	6.8 (10/147)	93.2 (137/147)
A9Gal4/+; UAS-cmpy(3), UAS-gbb(9.9)/+	89.4 (168/188)	10.6 (20/188)	0	0	88.7 (126/142)	11.3 (16/142)
A9Gal4/+; UAS-gbb(9.9), UAS-lacZ/+	21.7 (23/106)	78.3 (83/106)	0	0	17.2 (25/145)	82.8 (120/145)

*Actual numbers of flies showing the phenotype among the total examined is given in parentheses.
WT, wild type; B, blistered; B/U, blistered and unfurled.

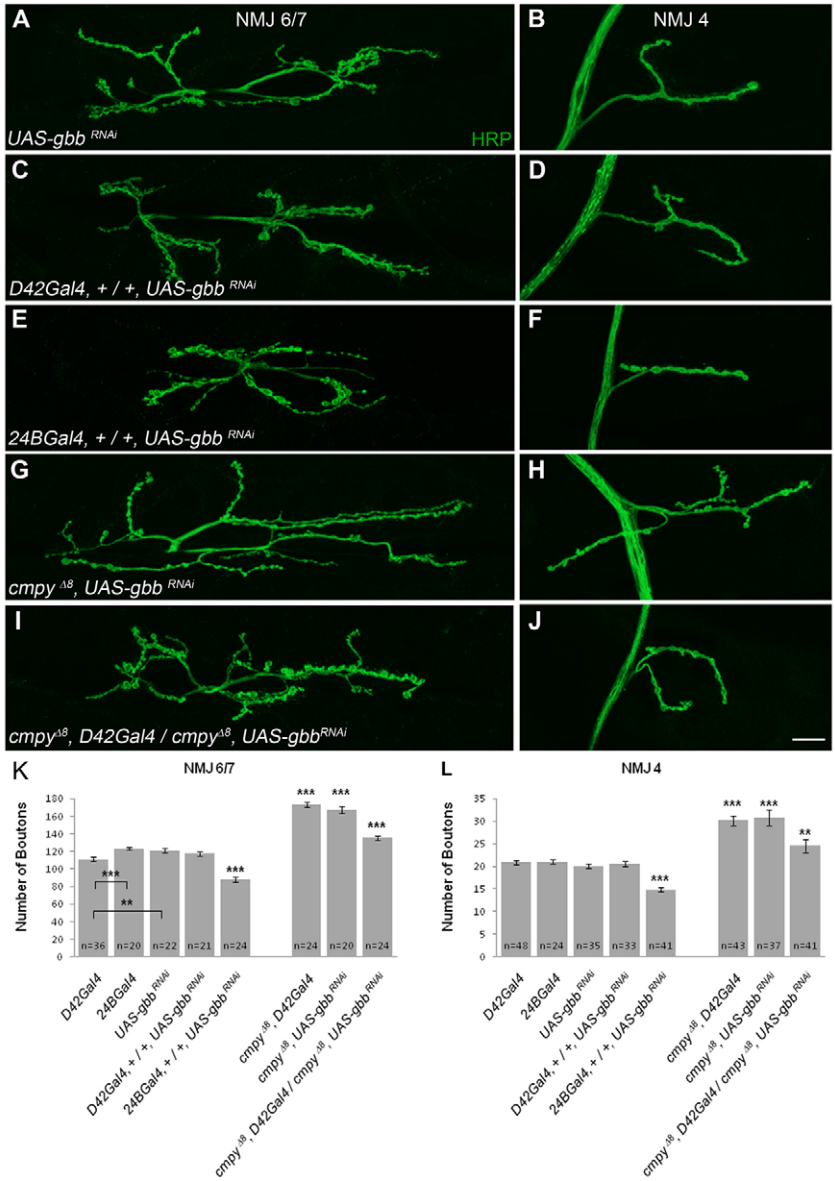

Fig. 6. RNAi-mediated knockdown of Gbb in motoneurons suppresses the *cmpy* loss-of-function phenotype. (**A-J**) Representative confocal images of *Drosophila* NMJ 6/7 (A,C,E,G,I) and NMJ 4 (B,D,F,H,J) labeled with anti-HRP. (A,B) Wild type corresponds to *UAS-gbb*^{RNAi}. (C,D) Motoneuronal knockdown of Gbb by RNAi does not affect bouton number at NMJ 6/7 or NMJ 4, whereas knockdown in muscle drives NMJ undergrowth (E,F). Motoneuronal knockdown of Gbb suppresses the NMJ overgrowth phenotypes observed at *cmpy* loss-of-function (LOF) NMJs (G-J). (**K**,**L**) Quantification of the mean number of type I boutons per genotype at NMJ 6/7 and NMJ 4. Statistical comparisons are to wild type unless otherwise indicated. Error bars represent s.e.m. **, $P<0.01$; ***, $P<0.001$. Raw data are found in Table 4. Scale bar: 20 μm.

Cmpy antagonizes motoneuron-derived Gbb at the NMJ

Our genetic analyses suggest that *cmpy* antagonizes BMP pathway activity in motoneurons. If so, the NMJ overgrowth observed in *cmpy* LOF mutants should be suppressed by RNAi-mediated knockdown of Gbb in motoneurons. We first tested whether motoneuronal Gbb is necessary for normal NMJ growth by driving *UAS-gbb*^{RNAi} (Ballard et al., 2010) in motoneurons using the *D42Gal4* driver. *D42Gal4/UAS-gbb*^{RNAi} larvae displayed wild-type numbers of boutons at NMJ 6/7 and NMJ 4 (Fig. 6A-D,K,L; Table 4), suggesting that motoneuron-derived Gbb does not regulate bouton number. Supporting this conclusion, neuronal *cmpy* overexpression driven with either *elavGal4* or *D42Gal4* had no effect on bouton number (Table 2; data not shown). These data argue that presynaptic Gbb does not play a role in NMJ growth regulation. To investigate the efficacy of the *gbb*^{RNAi} construct, we also expressed it postsynaptically. *24BGal4/UAS-gbb*^{RNAi} animals displayed a 28% decrease in bouton number at both NMJ 6/7 and NMJ 4 (Fig. 6E,F,K,L; Table 4), providing evidence that *UAS-gbb*^{RNAi} inhibits Gbb expression. This experiment also establishes that muscle-derived Gbb is necessary for proper regulation of NMJ expansion.

We next assessed whether motoneuronal expression of *gbb*^{RNAi} modulates the NMJ overgrowth in *cmpy* LOF mutants. Driving *gbb*^{RNAi} using *D42Gal4* in a *cmpy* homozygous mutant background strongly suppressed the *cmpy* LOF mutant phenotype. RNAi-mediated knockdown of Gbb in motoneurons in *cmpy* mutants suppressed the NMJ overgrowth from 46% to 16% at NMJ 6/7 and from 49% to 20% at NMJ 4 (Fig. 6G-L; Table 4). These results indicate that Cmpy inhibits the motoneuron-derived pool of Gbb at the NMJ.

Since Gbb is normally secreted from the postsynaptic muscle, muscle-specific Cmpy misexpression is predicted to interfere with NMJ growth. Utilizing *24BGal4* to drive *cmpy* misexpression in muscle, we observed a 20% decrease in type I boutons at NMJ 6/7 and a 22% decrease at NMJ 4 (Table 2). Comparable results were obtained with a second *UAS-cmpy* line (data not shown). Thus, muscle-specific Cmpy misexpression drives NMJ undergrowth, consistent with the model that Cmpy antagonizes Gbb.

Table 4. *gbb* RNAi phenotypes at the NMJ

Genotype	NMJ 6/7 (A2)		NMJ 4 (A2 + A3)	
	n	Total boutons	*n*	Total boutons
D42Gal4	36	111.3±2.0	48	20.9±0.4
24BGal4	20	123.0±1.9	24	21.0±0.4
UAS-gbb^{RNAi}	22	121.2±2.1	35	20.1±0.5
D42Gal4, +/+, UAS-gbb^{RNAi}	21	117.4±2.2	33	20.6±0.5
24BGal4, +/+, UAS-gbb^{RNAi}	24	88.2±3.0	41	14.9±0.5
cmpy$^{\Delta 8}$, D42Gal4	24	172.9±3.1	43	30.1±1.1
cmpy$^{\Delta 8}$, UAS-gbb^{RNAi}	20	167.3±4.1	37	30.8±1.7
cmpy$^{\Delta 8}$, D42Gal4/cmpy$^{\Delta 8}$, UAS-gbb^{RNAi}	24	135.3±2.7	41	24.5±1.4

n, the number of NMJs scored per genotype; data represent two or more experiments pooled.

Cmpy physically interacts with the Gbb precursor protein

BMP activity is regulated at multiple levels, including processing, secretion and receptor binding (Umulis et al., 2009; Walsh et al., 2010). BMPs are synthesized as precursor proteins that are cleaved by endopeptidases into prodomain and signaling fragments (Constam and Robertson, 1999; Cui et al., 1998; Kunnapuu et al., 2009). After processing, the prodomain remains non-covalently associated with the mature signaling fragment and may serve a regulatory function (Cui et al., 1998; Degnin et al., 2004). Additionally, CRR-containing BMP antagonists, including vertebrate chordin and noggin and *Drosophila* Sog, predominantly inhibit BMP activity by binding to BMPs and blocking ligand-receptor interactions (Umulis et al., 2009; Walsh et al., 2010).

To test whether Cmpy and Gbb associate in a complex, we performed co-immunoprecipitation experiments from S2 cell lysates. Indeed, C-terminal epitope-tagged Cmpy-Flag and Gbb-HA proteins co-immunoprecipitated (Fig. 7A). Cmpy immunoprecipitated unprocessed Gbb (55 kDa), indicating that Cmpy associates with full-length Gbb precursor protein. Gbb also immunoprecipitated Cmpy (Fig. 7A). We detected two forms of Cmpy in these experiments: a 33 kDa form, consistent with full-

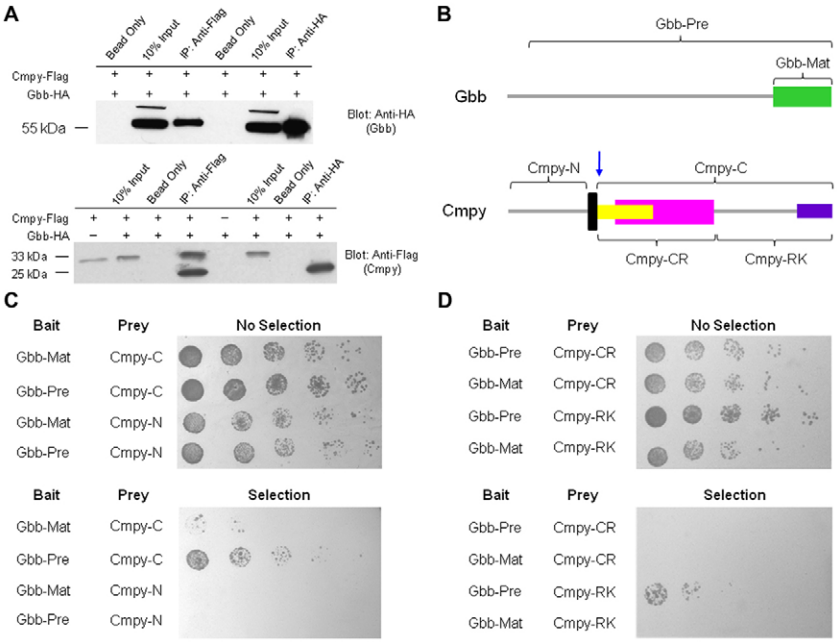

Fig. 7. Cmpy physically interacts with the Gbb precursor protein. (**A**) Immunoprecipitation from *Drosophila* S2R+ cell lysates demonstrates that C-terminal tagged Cmpy-Flag and Gbb-HA fusion proteins form a complex. (Top) Both anti-Flag (Cmpy) and anti-HA (Gbb) precipitate full-length, unprocessed Gbb (55 kDa). (Bottom) Anti-Flag antibody (Cmpy) precipitates both full-length Cmpy (33 kDa) and a processed, smaller Cmpy form (25 kDa). Anti-HA (Gbb) precipitates only the smaller Cmpy isoform. (**B**) Domains of Cmpy and Gbb used to analyze interaction by yeast two-hybrid. Gbb-Pre is the precursor form of Gbb, including the prodomain and the mature ligand Gbb-Mat. Cmpy-N is the region of Cmpy N-terminal to the transmembrane domain (black), and Cmpy-C is the region of Cmpy C-terminal to the transmembrane domain, including most of the CRR (yellow), the IGFBP domain (magenta) and the arginine/lysine-rich region (purple). The blue arrow indicates the approximate location of the proposed proteolytic processing of Cmpy as indicated by the molecular weight of the smaller Cmpy isoform in A. (**C**) Yeast two-hybrid interactions demonstrate a physical interaction between Cmpy and Gbb. Gbb-Mat and Gbb-Pre are fused to the GAL4 DNA-binding domain (bait), whereas Cmpy-N and Cmpy-C are fused to the GAL4 activation domain (prey). Cmpy-C interacts strongly with Gbb-Pre and weakly with Gbb-Mat. Cmpy-N does not interact with either region of Gbb in this assay. (**D**) Yeast two-hybrid analysis demonstrates that the C-terminal portion of Cmpy containing the arginine/lysine-rich region (Cmpy-RK), but not the CRR region (Cmpy-CR), interacts with Gbb-Pre.

length protein, and a smaller 25 kDa form (Fig. 7A). The smaller isoform suggests that Cmpy is proteolytically processed, and its molecular weight suggests a cleavage site immediately C-terminal to the predicted transmembrane domain (arrow in Fig. 7B). Gbb selectively associates with the smaller 25 kDa Cmpy isoform, arguing that Gbb interacts preferentially with processed Cmpy. Thus, Cmpy and Gbb can associate in a complex. Furthermore, since Cmpy associates with the precursor form of Gbb, these experiments suggest that Cmpy binds Gbb prior to the generation of mature ligand.

We used a yeast interaction assay to verify the relevant protein interaction domains and assess the likelihood that the Cmpy-Gbb association is direct. We tested N- and C-terminal fragments of Cmpy and found that the C-terminal Cmpy fragment (Cmpy-C) interacts with Gbb (Fig. 7B,C), consistent with the 25 kDa Cmpy isoform that co-immunoprecipitates with Gbb. Furthermore, the precursor form of Gbb (Gbb-Pre) interacted robustly with Cmpy in yeast, whereas processed/mature Gbb (Gbb-Mat) interacted only weakly (Fig. 7B,C). We next subdivided the Cmpy-C fragment into a fragment containing the CRR (Cmpy-CR) and a fragment containing the arginine/lysine-rich region (Cmpy-RK). Surprisingly, the Cmpy-RK fragment interacted with Gbb-Pre, whereas Cmpy-CR interacted with neither Gbb-Pre nor Gbb-Mat (Fig. 7B,D), suggesting that the Cmpy-Gbb interaction is mediated by sequences outside of the CRR. These data support the co-immunoprecipitation results and indicate that Cmpy binds the unprocessed, precursor form of Gbb, which is in line with the model that Cmpy interacts with Gbb prior to ligand processing.

Together, the experiments presented here indicate that Cmpy inhibits Gbb in motoneurons, thus contributing to the retrograde directionality of the pro-growth BMP signal at the NMJ.

DISCUSSION

Gbb has been proposed to cue presynaptic motoneurons to the size of their postsynaptic muscle partners. However, muscles have not been established as the primary source of Gbb at the NMJ. In fact, motoneuron-derived Gbb has a crucial retrograde activity at the motoneuron-interneuron synapse (Baines, 2004), demonstrating that motoneuronal Gbb is active. In the present work, we demonstrate that motoneurons express Cmpy, a Gbb antagonist. We propose that Cmpy restrains motoneuronal activity of Gbb at the NMJ, thus establishing the muscle as the predominant source of the pro-growth BMP signal. Here, we discuss potential mechanisms for Cmpy function at the NMJ and the relationship of Cmpy with intracellular and extracellular BMP antagonists.

Our interest in CG13253/Crimpy was sparked by its restricted expression in the VNC and was reinforced by the presence of a predicted transmembrane domain and CRR. The presence of these two sequence elements renders Cmpy similar to vertebrate Crim1 (Kolle et al., 2000; Kolle et al., 2003). In mice, Crim1 hypomorphs have been described and display pleiotropic defects in multiple organ systems (Pennisi et al., 2007). Notably, Crim1 is expressed in developing motoneuron and interneuron populations in the developing mouse and chick spinal cord, although LOF studies have not addressed a neuronal function. A Crim1 homolog has also been described in zebrafish, where it is linked to vascular and somitic development (Kinna et al., 2006), and in *C. elegans*, where RNAi-mediated knockdown of *crm-1* (*cysteine-rich motor neuron protein 1*) suggests a pro-BMP function in the control of body size (Fung et al., 2007). Cell culture studies provide evidence that Crim1 binds Bmp4/7 and antagonizes the production and processing of the preprotein in the Golgi (Wilkinson et al., 2003). Interestingly, these authors also demonstrated that Crim1 interacts with Bmp4/7 at the cell surface and inhibits BMP secretion into the medium (Wilkinson et al., 2003), raising the possibility that Crim1 antagonizes BMP signaling by multiple cellular mechanisms.

CRR-containing proteins are established modulators of BMP signaling in vertebrates and invertebrates. In *Drosophila*, posterior wing crossvein specification requires local activation of the BMP pathway, and loss of BMP signaling yields a crossveinless phenotype (Conley et al., 2000). BMP ligands are produced in neighboring longitudinal wing veins and are transported to the posterior crossvein (Ralston and Blair, 2005; Ray and Wharton, 2001). Ligand activity is differentially regulated by the secreted CRR-containing proteins Sog and Crossveinless 2 (Cv-2). Sog and Cv-2 both have pro- and anti-BMP activity, although their mode and range of action differ (Serpe et al., 2005; Serpe et al., 2008; Shimmi et al., 2005a). Sog is proposed to act at long range, and its anti-BMP activity is thought to derive from sequestering BMPs from their receptors, whereas its pro-BMP activity is likely to arise from transporting BMP ligands through tissues (Serpe et al., 2005; Shimmi et al., 2005a; Shimmi et al., 2005b). By contrast, Cv-2 is proposed to act at short range and binds heparan sulfate proteoglycans and the type I receptor Tkv.

The biphasic activities of Sog and Cv-2 serve to emphasize the complex modes of extracellular regulation of BMPs by CRR-containing proteins, as well as to draw attention to possible differences between BMP regulation in the wing and Cmpy-dependent BMP regulation at the NMJ. Although overexpression of Cmpy suppresses Gbb overexpression phenotypes in the wing, *cmpy* LOF mutants do not display wing vein phenotypes (R.E.J. and H.T.B., unpublished data). Cmpy does not function during early embryogenesis, when the BMP homolog Decapentaplegic acts as a classical morphogen in dorsoventral patterning (Decotto and Ferguson, 2001; Francois et al., 1994). In both the early embryo and the wing, BMP activity is shaped over many cell diameters by extracellular CRR-containing proteins. As discussed above, Sog and Cv-2 play essential extracellular roles in establishing the magnitude and directionality of BMP signaling. By contrast, Gbb is proposed to act locally at the NMJ to couple pre- and postsynaptic growth.

The close apposition of the cells that send and receive BMP at the NMJ might relieve a requirement for long-range extracellular regulation of the ligand. Instead, we propose that a primary challenge at the NMJ is to establish the cellular source of the BMP signal, as Gbb is present both in motoneurons and muscle (Baines, 2004; McCabe et al., 2003; Wharton et al., 1999). In this case, cell-autonomous regulation of the ligand could provide a mechanism for the motoneuron to discriminate between motoneuron- and muscle-derived pools. Consistent with this model, we have presented evidence that Cmpy binds Gbb prior to processing and inhibits its growth-promoting activity in motoneurons. In this manner, the Cmpy-Gbb interaction might provide motoneurons with an effective mechanism for distinguishing autocrine and paracrine Gbb signals within the NMJ microenvironment.

CRR-containing BMP antagonists were initially identified from their extracellular roles in the establishment of BMP morphogenetic gradients (Garcia Abreu et al., 2002; Zakin and De Robertis, 2010). It will be interesting to determine whether additional CRR-containing proteins function intracellularly as more short-range BMP-dependent signaling interactions are thoroughly described. Consistent with this idea, several mammalian CRR-containing proteins bind precursor forms of BMP and inhibit BMP

activity or secretion in a cell-autonomous manner (Krause et al., 2010; Sun et al., 2006). Gremlin is a BMP antagonist that is expressed in differentiated cells, including neurons (Topol et al., 1997). When co-expressed with Bmp4, gremlin binds to the precursor form of Bmp4 and inhibits secretion (Sun et al., 2006). sclerostin, another BMP antagonist, inhibits Bmp7 secretion when the proteins are co-expressed in osteocytes (Krause et al., 2010). These studies argue that intracellular modulation of ligand production contributes to BMP signaling directionality in vertebrates.

The work presented here suggests that Cmpy antagonizes Gbb activity in motoneurons prior to ligand secretion. To further delineate the Cmpy-Gbb relationship, it will be important to map their localization patterns in motoneurons using compartment-specific markers. Although attempts to generate anti-Cmpy antibodies have been unsuccessful (R.E.J. and H.T.B., unpublished data), generation of transgenic flies carrying epitope-tagged Cmpy might enable an analysis of Cmpy subcellular localization. Cmpy-mediated inhibition of Gbb at the NMJ might rely upon restricted localization of Cmpy to this subcellular locale; however, the possibility that Cmpy regulates Gbb activity at the central synapse remains open. Investigation of the localization pattern of Cmpy in motoneurons will begin to address the issue of Cmpy function at these distinct synapses.

An analysis of Gbb distribution, trafficking and secretion in motoneurons in *cmpy* mutants will indicate the stage of Gbb processing at which Cmpy is likely to act. Studies on mammalian sclerostin provide precedent for an intracellular mechanism for BMP inhibition, as sclerostin sequesters Bmp7 preprotein, leading to its intracellular retention and proteasomal degradation (Krause et al., 2010). Interestingly, Cmpy contains only a single, low-threshold CRR. These motifs modulate interactions with mature secreted ligand (Walsh et al., 2010), suggesting that sequences outside of the CRR mediate interactions with the precursor form of Gbb. Indeed, interaction of Cmpy with Gbb is dependent on C-terminal sequences, including an arginine/lysine-rich domain at the extreme C-terminus. Likewise, the intracellular interaction of gremlin with the precursor form of Bmp4 is not modulated by its cysteine-rich region, but rather by an arginine/lysine-rich domain (Sun et al., 2006). The sequence similarities between the BMP interaction domains in gremlin and Crimpy raise the possibility that these proteins antagonize BMP activity by a conserved mechanism.

We have focused here on Cmpy regulation of Gbb in the anatomical development of the NMJ. In addition, Gbb regulates baseline neurotransmission and synaptic homeostasis at the NMJ (Goold and Davis, 2007). Motoneurons precisely compensate for impaired postsynaptic neurotransmitter receptor sensitivity by increasing presynaptic neurotransmitter release (Frank et al., 2006; Petersen et al., 1997). This homeostatic response requires Gbb, which is not itself the acute retrograde homeostatic signal but rather establishes the competence of motoneurons to receive the homeostatic signal (Goold and Davis, 2007). A number of genetic manipulations indicate that the roles of Gbb in regulating synaptic homeostasis, basal neurotransmission and NMJ morphology are separable. Perhaps surprisingly, neuron-specific Gbb rescues both synaptic homeostasis and baseline neurotransmitter release in *gbb* null animals. By contrast, whereas muscle-derived Gbb rescues synaptic homeostasis in *gbb* null animals, it does not significantly rescue baseline synaptic function (Goold and Davis, 2007), arguing that neuronal- and muscle-derived pools of Gbb serve distinct functions. Although our data indicate that Cmpy antagonizes autocrine Gbb signaling in motoneurons to restrain morphological expansion at the NMJ, it is likely that motoneuronal Gbb has an independent role in regulating functional development of the NMJ. If so, the Cmpy-Gbb complex might be active and could elicit a signaling outcome distinct from that of the muscle-derived pool of Gbb. Physiological analyses of *cmpy* mutants, as well as an investigation of Gbb trafficking and secretion at the NMJ in *cmpy* mutants, should provide crucial insight into this important question.

More broadly, this study is of relevance to the regulation of signal release in neurons. By definition, neurotransmitter is released from the presynaptic compartment and received by neurotransmitter receptors on the postsynaptic side. However, signaling pathway activity is not circumscribed in this way and may occur at short or long range at multiple subcellular positions. Hence, neurons are likely to possess fine-regulatory mechanisms controlling the release of, and response to, extracellular cues. The present work provides insight into the regulation of signaling molecules in neurons and suggests that we are only beginning to uncover the mechanisms that control signaling specificity in the developing nervous system.

Acknowledgements

We thank Nan Liu and Chris Dejelo for excellent technical assistance; K. O'Connor-Giles, A. Page-McCaw and members of the H.T.B. lab for intellectual input and comments on the manuscript; and the Bloomington Stock Center, the Developmental Studies Hybridoma Bank, A. DiAntonio, B. McCabe, K. O'Connor-Giles and K. Wharton for antibodies and/or fly stocks. This work was supported by NIH RO1NS055245 and the Mt Sinai Foundation to H.T.B., and by NIH T32 AG00271 and NIH T32 HD-07104-31 to R.E.J. Deposited in PMC for release after 12 months.

Competing interests statement

The authors declare no competing financial interests.

References

Aberle, H., Haghighi, A. P., Fetter, R. D., McCabe, B. D., Magalhaes, T. R. and Goodman, C. S. (2002). wishful thinking encodes a BMP type II receptor that regulates synaptic growth in Drosophila. *Neuron* **33**, 545-558.

Allan, D. W., St Pierre, S. E., Miguel-Aliaga, I. and Thor, S. (2003). Specification of neuropeptide cell identity by the integration of retrograde BMP signaling and a combinatorial transcription factor code. *Cell* **113**, 73-86.

Ataman, B., Ashley, J., Gorczyca, M., Ramachandran, P., Fouquet, W., Sigrist, S. J. and Budnik, V. (2008). Rapid activity-dependent modifications in synaptic structure and function require bidirectional Wnt signaling. *Neuron* **57**, 705-718.

Atwood, H. L., Govind, C. K. and Wu, C. F. (1993). Differential ultrastructure of synaptic terminals on ventral longitudinal abdominal muscles in Drosophila larvae. *J. Neurobiol.* **24**, 1008-1024.

Bachiller, D., Klingensmith, J., Kemp, C., Belo, J. A., Anderson, R. M., May, S. R., McMahon, J. A., McMahon, A. P., Harland, R. M., Rossant, J. et al. (2000). The organizer factors Chordin and Noggin are required for mouse forebrain development. *Nature* **403**, 658-661.

Baines, R. A. (2004). Synaptic strengthening mediated by bone morphogenetic protein-dependent retrograde signaling in the Drosophila CNS. *J. Neurosci.* **24**, 6904-6911.

Ballard, S. L., Jarolimova, J. and Wharton, K. A. (2010). Gbb/BMP signaling is required to maintain energy homeostasis in Drosophila. *Dev. Biol.* **337**, 375-385.

Brand, A. H. and Perrimon, N. (1993). Targeted gene expression as a means of altering cell fates and generating dominant phenotypes. *Development* **118**, 401-415.

Broihier, H. T. and Skeath, J. B. (2002). Drosophila homeodomain protein dHb9 directs neuronal fate via crossrepressive and cell-nonautonomous mechanisms. *Neuron* **35**, 39-50.

Collins, C. A. and DiAntonio, A. (2007). Synaptic development: insights from Drosophila. *Curr. Opin. Neurobiol.* **17**, 35-42.

Conley, C. A., Silburn, R., Singer, M. A., Ralston, A., Rohwer-Nutter, D., Olson, D. J., Gelbart, W. and Blair, S. S. (2000). Crossveinless 2 contains cysteine-rich domains and is required for high levels of BMP-like activity during the formation of the cross veins in Drosophila. *Development* **127**, 3947-3959.

Constam, D. B. and Robertson, E. J. (1999). Regulation of bone morphogenetic protein activity by pro domains and proprotein convertases. *J. Cell Biol.* **144**, 139-149.

Cui, Y., Jean, F., Thomas, G. and Christian, J. L. (1998). BMP-4 is proteolytically activated by furin and/or PC6 during vertebrate embryonic development. *EMBO J.* **17**, 4735-4743.

Decotto, E. and Ferguson, E. L. (2001). A positive role for Short gastrulation in modulating BMP signaling during dorsoventral patterning in the Drosophila embryo. *Development* **128**, 3831-3841.
Degnin, C., Jean, F., Thomas, G. and Christian, J. L. (2004). Cleavages within the prodomain direct intracellular trafficking and degradation of mature bone morphogenetic protein-4. *Mol. Biol. Cell* **15**, 5012-5020.
Dickman, D. K., Lu, Z., Meinertzhagen, I. A. and Schwarz, T. L. (2006). Altered synaptic development and active zone spacing in endocytosis mutants. *Curr. Biol.* **16**, 591-598.
Dudu, V., Bittig, T., Entchev, E., Kicheva, A., Julicher, F. and Gonzalez-Gaitan, M. (2006). Postsynaptic mad signaling at the Drosophila neuromuscular junction. *Curr. Biol.* **16**, 625-635.
Francois, V., Solloway, M., O'Neill, J. W., Emery, J. and Bier, E. (1994). Dorsal-ventral patterning of the Drosophila embryo depends on a putative negative growth factor encoded by the short gastrulation gene. *Genes Dev.* **8**, 2602-2616.
Frank, C. A., Kennedy, M. J., Goold, C. P., Marek, K. W. and Davis, G. W. (2006). Mechanisms underlying the rapid induction and sustained expression of synaptic homeostasis. *Neuron* **52**, 663-677.
Fung, W. Y., Fat, K. F., Eng, C. K. and Lau, C. K. (2007). crm-1 facilitates BMP signaling to control body size in Caenorhabditis elegans. *Dev. Biol.* **311**, 95-105.
Garcia Abreu, J., Coffinier, C., Larrain, J., Oelgeschlager, M. and De Robertis, E. M. (2002). Chordin-like CR domains and the regulation of evolutionarily conserved extracellular signaling systems. *Gene* **287**, 39-47.
Goold, C. P. and Davis, G. W. (2007). The BMP ligand Gbb gates the expression of synaptic homeostasis independent of synaptic growth control. *Neuron* **56**, 109-123.
Johansen, J., Halpern, M. E., Johansen, K. M. and Keshishian, H. (1989). Stereotypic morphology of glutamatergic synapses on identified muscle cells of Drosophila larvae. *J. Neurosci.* **9**, 710-725.
Keshishian, H. and Kim, Y. S. (2004). Orchestrating development and function: retrograde BMP signaling in the Drosophila nervous system. *Trends Neurosci.* **27**, 143-147.
Khalsa, O., Yoon, J. W., Torres-Schumann, S. and Wharton, K. A. (1998). TGF-beta/BMP superfamily members, Gbb-60A and Dpp, cooperate to provide pattern information and establish cell identity in the Drosophila wing. *Development* **125**, 2723-2734.
Kim, S., Wairkar, Y. P., Daniels, R. W. and DiAntonio, A. (2010). The novel endosomal membrane protein Ema interacts with the class C Vps-HOPS complex to promote endosomal maturation. *J. Cell Biol.* **188**, 717-734.
Kinna, G., Kolle, G., Carter, A., Key, B., Lieschke, G. J., Perkins, A. and Little, M. H. (2006). Knockdown of zebrafish crim1 results in a bent tail phenotype with defects in somite and vascular development. *Mech. Dev.* **123**, 277-287.
Kolle, G., Georgas, K., Holmes, G. P., Little, M. H. and Yamada, T. (2000). CRIM1, a novel gene encoding a cysteine-rich repeat protein, is developmentally regulated and implicated in vertebrate CNS development and organogenesis. *Mech. Dev.* **90**, 181-193.
Kolle, G., Jansen, A., Yamada, T. and Little, M. (2003). In ovo electroporation of Crim1 in the developing chick spinal cord. *Dev. Dyn.* **226**, 107-111.
Krause, C., Korchynskyi, O., de Rooij, K., Weidauer, S. E., de Gorter, D. J., van Bezooijen, R. L., Hatsell, S., Economides, A. N., Mueller, T. D., Lowik, C. W. et al. (2010). Distinct modes of inhibition by sclerostin on bone morphogenetic protein and Wnt signaling pathways. *J. Biol. Chem.* **285**, 41614-41626.
Kunnapuu, J., Bjorkgren, I. and Shimmi, O. (2009). The Drosophila DPP signal is produced by cleavage of its proprotein at evolutionary diversified furin-recognition sites. *Proc. Natl. Acad. Sci. USA* **106**, 8501-8506.
Lahey, T., Gorczyca, M., Jia, X. X. and Budnik, V. (1994). The Drosophila tumor suppressor gene dlg is required for normal synaptic bouton structure. *Neuron* **13**, 823-835.
Landgraf, M., Roy, S., Prokop, A., VijayRaghavan, K. and Bate, M. (1999). even-skipped determines the dorsal growth of motor axons in Drosophila. *Neuron* **22**, 43-52.
Marques, G., Bao, H., Haerry, T. E., Shimell, M. J., Duchek, P., Zhang, B. and O'Connor, M. B. (2002). The Drosophila BMP type II receptor Wishful Thinking regulates neuromuscular synapse morphology and function. *Neuron* **33**, 529-543.
Marrus, S. B., Portman, S. L., Allen, M. J., Moffat, K. G. and DiAntonio, A. (2004). Differential localization of glutamate receptor subunits at the Drosophila neuromuscular junction. *J. Neurosci.* **24**, 1406-1415.
McCabe, B. D., Marques, G., Haghighi, A. P., Fetter, R. D., Crotty, M. L., Haerry, T. E., Goodman, C. S. and O'Connor, M. B. (2003). The BMP homolog Gbb provides a retrograde signal that regulates synaptic growth at the Drosophila neuromuscular junction. *Neuron* **39**, 241-254.
McCabe, B. D., Hom, S., Aberle, H., Fetter, R. D., Marques, G., Haerry, T. E., Wan, H., O'Connor, M. B., Goodman, C. S. and Haghighi, A. P. (2004). Highwire regulates presynaptic BMP signaling essential for synaptic growth. *Neuron* **41**, 891-905.
Miech, C., Pauer, H. U., He, X. and Schwarz, T. L. (2008). Presynaptic local signaling by a canonical wingless pathway regulates development of the Drosophila neuromuscular junction. *J. Neurosci.* **28**, 10875-10884.
Miller, C. M., Page-McCaw, A. and Broihier, H. T. (2008). Matrix metalloproteinases promote motor axon fasciculation in the Drosophila embryo. *Development* **135**, 95-109.
O'Connor-Giles, K., Ho, L. and Ganetzky, B. (2008). Nervous Wreck interacts with Thickveins and the endocytic machinery to attenuate retrograde BMP signaling during synaptic growth. *Neuron* **58**, 507-518.
Odden, J. P., Holbrook, S. and Doe, C. Q. (2002). Drosophila HB9 is expressed in a subset of motoneurons and interneurons, where it regulates gene expression and axon pathfinding. *J. Neurosci.* **22**, 9143-9149.
Packard, M., Koo, E. S., Gorczyca, M., Sharpe, J., Cumberledge, S. and Budnik, V. (2002). The Drosophila Wnt, wingless, provides an essential signal for pre- and postsynaptic differentiation. *Cell* **111**, 319-330.
Parks, A. L., Cook, K. R., Belvin, M., Dompe, N. A., Fawcett, R., Huppert, K., Tan, L. R., Winter, C. G., Bogart, K. P., Deal, J. E. et al. (2004). Systematic generation of high-resolution deletion coverage of the Drosophila melanogaster genome. *Nat. Genet.* **36**, 288-292.
Pennisi, D. J., Wilkinson, L., Kolle, G., Sohaskey, M. L., Gillinder, K., Piper, M. J., McAvoy, J. W., Lovicu, F. J. and Little, M. H. (2007). Crim1KST264/KST264 mice display a disruption of the Crim1 gene resulting in perinatal lethality with defects in multiple organ systems. *Dev. Dyn.* **236**, 502-511.
Petersen, S. A., Fetter, R. D., Noordermeer, J. N., Goodman, C. S. and DiAntonio, A. (1997). Genetic analysis of glutamate receptors in Drosophila reveals a retrograde signal regulating presynaptic transmitter release. *Neuron* **19**, 1237-1248.
Raftery, L. A. and Sutherland, D. J. (1999). TGF-beta family signal transduction in Drosophila development: from Mad to Smads. *Dev. Biol.* **210**, 251-268.
Ralston, A. and Blair, S. S. (2005). Long-range Dpp signaling is regulated to restrict BMP signaling to a crossvein competent zone. *Dev. Biol.* **280**, 187-200.
Rawson, J. M., Lee, M., Kennedy, E. L. and Selleck, S. B. (2003). Drosophila neuromuscular synapse assembly and function require the TGF-beta type I receptor saxophone and the transcription factor Mad. *J. Neurobiol.* **55**, 134-150.
Ray, R. P. and Wharton, K. A. (2001). Context-dependent relationships between the BMPs gbb and dpp during development of the Drosophila wing imaginal disk. *Development* **128**, 3913-3925.
Rossignol, P., Collier, S., Bush, M., Shaw, P. and Doonan, J. H. (2007). Arabidopsis POT1 interacts with TERT-V(18), an N-terminal splicing variant of telomerase. *J. Cell Sci.* **120**, 3678-3687.
Sanyal, S. (2009). Genomic mapping and expression patterns of C380, OK6 and D42 enhancer trap lines in the larval nervous system of Drosophila. *Gene Expr. Patterns* **9**, 371-380.
Serpe, M., Ralston, A., Blair, S. S. and O'Connor, M. B. (2005). Matching catalytic activity to developmental function: tolloid-related processes Sog in order to help specify the posterior crossvein in the Drosophila wing. *Development* **132**, 2645-2656.
Serpe, M., Umulis, D., Ralston, A., Chen, J., Olson, D. J., Avanesov, A., Othmer, H., O'Connor, M. B. and Blair, S. S. (2008). The BMP-binding protein Crossveinless 2 is a short-range, concentration-dependent, biphasic modulator of BMP signaling in Drosophila. *Dev. Cell* **14**, 940-953.
Shimmi, O., Ralston, A., Blair, S. S. and O'Connor, M. B. (2005a). The crossveinless gene encodes a new member of the Twisted gastrulation family of BMP-binding proteins which, with Short gastrulation, promotes BMP signaling in the crossveins of the Drosophila wing. *Dev. Biol.* **282**, 70-83.
Shimmi, O., Umulis, D., Othmer, H. and O'Connor, M. B. (2005b). Facilitated transport of a Dpp/Scw heterodimer by Sog/Tsg leads to robust patterning of the Drosophila blastoderm embryo. *Cell* **120**, 873-886.
Sun, J., Zhuang, F. F., Mullersman, J. E., Chen, H., Robertson, E. J., Warburton, D., Liu, Y. H. and Shi, W. (2006). BMP4 activation and secretion are negatively regulated by an intracellular gremlin-BMP4 interaction. *J. Biol. Chem.* **281**, 29349-29356.
Sweeney, S. T. and Davis, G. W. (2002). Unrestricted synaptic growth in spinster-a late endosomal protein implicated in TGF-beta-mediated synaptic growth regulation. *Neuron* **36**, 403-416.
Thibault, S. T., Singer, M. A., Miyazaki, W. Y., Milash, B., Dompe, N. A., Singh, C. M., Buchholz, R., Demsky, M., Fawcett, R. Francis-Lang, H. L. et al. (2004). A complementary transposon tool kit for Drosophila melanogaster using P and piggyBac. *Nat. Genet.* **36**, 283-287.
Topol, L. Z., Marx, M., Laugier, D., Bogdanova, N. N., Boubnov, N. V., Clausen, P. A., Calothy, G. and Blair, D. G. (1997). Identification of drm, a novel gene whose expression is suppressed in transformed cells and which can inhibit growth of normal but not transformed cells in culture. *Mol. Cell. Biol.* **17**, 4801-4810.
Umulis, D., O'Connor, M. B. and Blair, S. S. (2009). The extracellular regulation of bone morphogenetic protein signaling. *Development* **136**, 3715-3728.
Van Vactor, D., Sink, H., Fambrough, D., Tsoo, R. and Goodman, C. S. (1993). Genes that control neuromuscular specificity in Drosophila. *Cell* **73**, 1137-1153.

Wagh, D. A., Rasse, T. M., Asan, E., Hofbauer, A., Schwenkert, I., Durrbeck, H., Buchner, S., Dabauvalle, M. C., Schmidt, M., Qin, G. et al. (2006). Bruchpilot, a protein with homology to ELKS/CAST, is required for structural integrity and function of synaptic active zones in Drosophila. *Neuron* **49**, 833-844.

Walsh, D. W., Godson, C., Brazil, D. P. and Martin, F. (2010). Extracellular BMP-antagonist regulation in development and disease: tied up in knots. *Trends Cell Biol.* **20**, 244-256.

Wang, X., Shaw, W. R., Tsang, H. T., Reid, E. and O'Kane, C. J. (2007). Drosophila spichthyin inhibits BMP signaling and regulates synaptic growth and axonal microtubules. *Nat. Neurosci.* **10**, 177-185.

Weng, Y. L., Liu, N., DiAntonio, A. and Broihier, H. T. (2011). The cytoplasmic adaptor protein Caskin mediates Lar signal transduction during Drosophila motor axon guidance. *J. Neurosci.* **31**, 4421-4433.

Wharton, K. A., Cook, J. M., Torres-Schumann, S., de Castro, K., Borod, E. and Phillips, D. A. (1999). Genetic analysis of the bone morphogenetic protein-related gene, gbb, identifies multiple requirements during Drosophila development. *Genetics* **152**, 629-640.

Wilkinson, L., Kolle, G., Wen, D., Piper, M., Scott, J. and Little, M. (2003). CRIM1 regulates the rate of processing and delivery of bone morphogenetic proteins to the cell surface. *J. Biol. Chem.* **278**, 34181-34188.

Zakin, L. and De Robertis, E. M. (2010). Extracellular regulation of BMP signaling. *Curr. Biol.* **20**, R89-R92.